Journal of Applied Polymer Science

Effect of electrical properties on gas sensitivity of polypyrrole/CdS nanocomposites

Bharati Yeole, Tanushree Sen, D. P. Hansora, Satyendra Mishra
Department of Plastics Technology, University Institute of Chemical Technology, North Maharashtra University, Jalgaon, India
Correspondence to: S. Mishra (E-mail: profsm@rediffmail.com)

ABSTRACT: In the present work, polypyrrole (PPy) nanocomposites were synthesized using ferric chloride ($FeCl_3$) as an oxidant by in situ polymerization at room temperature. Cadmium sulfide (CdS) nanoparticles were synthesized by ultrasonication technique with size ranging between 60 and 110 nm. The PPy/CdS nanocomposites were prepared by taking 1–3 wt % loading of CdS to measure the electrical conductivity. The PPy nanocomposites were characterized by using FTIR, X-ray diffraction, UV, and SEM. Furthermore, these PPy/CdS nanocomposites were investigated to study their effect of electrical properties on gas sensitivity of ammonia and LPG. The nanocomposites showed improvement in conductivity and sensing response toward 250 ppm NH_3 was found to be maximum (4.2) compared with 100 and 500 ppm NH_3 gas, whereas in the case of LPG, it showed sensitive response. © 2015 Wiley Periodicals, Inc. J. Appl. Polym. Sci. **2015**, *132*, 42379.

KEYWORDS: conducting polymers; nanoparticles; nanowires and nanocrystals; properties and characterization; sensors and actuators

Received 10 January 2015; accepted 19 April 2015
DOI: 10.1002/app.42379

INTRODUCTION

Conducting polymer-based nanocomposites possess improved physical and structural properties, which have been widely studied due to their potential applications as chemical sensors, electrochemical super capacitors, electro chromic devices, photovoltaic, light-emitting diodes, optical computers, and batteries.[1–9] Conducting polymer nanocomposites can be developed by incorporating inorganic nanomaterials *via* various methods.[5,10–19] Type of polymerization method, various oxidants, and temperature are crucial important parameters in terms of their physical and structural properties that can also play vital role in selection of most appropriate preparation method for composites.[14,17–21] Various technologies of nanoscience have been used for gas sensing[22–24] measurement. So far, various materials like metal oxides[25–27] and conducting polymers[6–8,28] are widely used for gas detection purpose. Ammonia gas has been successfully detected using various polymers, metal oxides,[15,29–32] and their composites.[33–38] Polymers encapsulated with metal nanocrystal can be used as a promoter for gas sensing at room temperature.[9]

Polypyrrole (PPy) can be one of the most extensively studied conducting polymers because of its high electrical conductivity and chemical stability. It can easily be prepared through chemical and electrochemical oxidation of pyrrole in the organic solvents and in aqueous medium.[1–8,10–14,17–19,33–43] Chemical polymerization is the preferred method in this study because it is a simple and fast process without any need of special instruments. The reaction of PPy with aqueous ferric chloride ($FeCl_3$) is rapid and the product is in the form of a black powder.[44] Iron (III) salts provide a convenient means for oxidative polymerizing PPy and incorporating their anions as dopant ions.[45] PPy° changed to PPy^{+} (H) spontaneously when it was dipped in an acidic aqueous solution, and it changed to PPy^{+} (OH) when dipped in an alkaline or neutral aqueous solution.[46] It has been noticed that factors such as solvent, reaction temperature, time, nature and concentration of the oxidizing agent, affect the oxidation potential of the solution. These in turn influence the final conductivity of the chemically synthesized PPy.[47,48] Nanoparticles and nanocomposites of cadmium sulfide (CdS) have been synthesized and studied for sensing and semiconductor behavior.[43,49,50] PPy/metal nanoparticle-based nanocomposites have also been investigated for gas sensing and electrical behavior.[1–5,10–14,17–19,33,36–43]

In this study, PPy/CdS nanocomposites were prepared by in situ polymerization with 1–3 wt % loading of CdS nanoparticles to measure the sensitivity of LPG and NH_3 gases. An effect of electrical properties on gas sensitivity of PPy/CdS nanocomposites has been also studied.

EXPERIMENTAL

Materials

Analytical grade pyrrole and $FeCl_3$ were purchased from Merck (Mumbai, India), whereas sodium lauryl sulfate (SLS) were

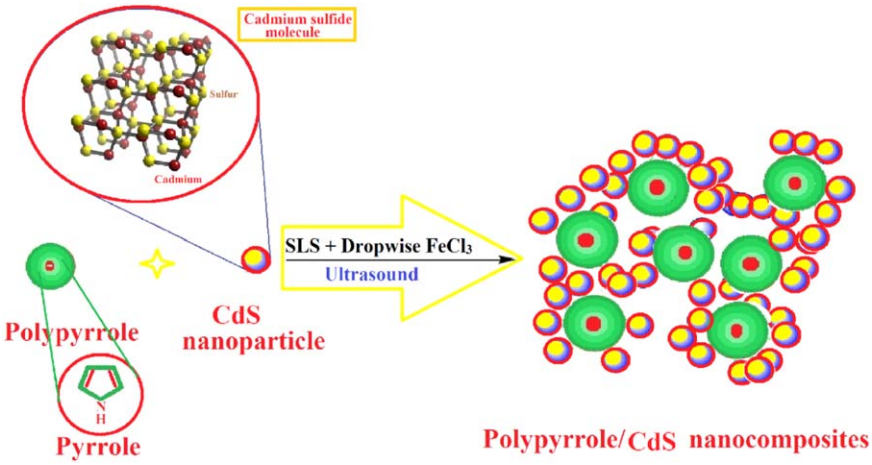

Figure 1. In situ chemical polymerization of PPy/CdS nanocomposites. [Color figure can be viewed in the online issue, which is available at wileyonlinelibrary.com.]

received from S.D. Fine Chem. (Mumbai, India). Cadmium nitrate ($CdNO_3$) was received from Loba Chemie (Mumbai, India), and sodium sulfide (Na_2S) was received from Himedia Laboratories Pvt. (Mumbai, India). Ultra-pure water from Smart 2 Pure system (Thermo Electron LED GmbH, Germany) was used for preparing solutions, cleaning, and washing purpose. Acetone, Methanol (S.D. Fine Chem., Mumbai) were used for washing purpose. Ammonia gas was purchased from Master specialty gases Pvt. (Mumbai, India).

Treatment of Glass Slides

To prepare the glass slides for thin film deposition, the microscope glass slides (Polar India Corporation, Mumbai) were cleaned by immersing them completely in 0.1*M* HCl solution for an hour. The slides were then successively sonicated in water and methanol for 15 min each, followed by vacuum drying.

Synthesis of PPy by Chemical Polymerization

Here, in situ chemical polymerization route[14] was applied to prepare PPy and its nanostructures in the aqueous medium at the room temperature for 2 h using $FeCl_3$ as the oxidant. In this method, solution of 0.2*M* of pyrrole and 0.466*M* of $FeCl_3$ were prepared in 100 mL distilled water. The mole ratio of monomer to oxidant was kept (1 : 2.33) because it affects the quality of the resulting polymer films.[44] During chemical polymerization of pyrrole, electro neutrality of the polymer matrix is maintained by incorporation of anions from the reaction mixture. These counter ions are usually the anion of the chemical oxidant, *i.e.*, reduced product of oxidant, so $FeCl_3$ or Cl_2 are used as oxidants, where Cl^- iron is incorporated as counter ion.[1–5,11,12,20,33–35,39]

Solution of 0.2*M* pyrrole stirred continuously on magnetic stirrer at 400 rpm and 0.466*M* $FeCl_3$ was added drop wise as one drop per second. The films formed in $FeCl_3$ solution are blue–black in color if that are fully oxidized. Induction time was noted. After completion of 2 h reaction, the solution was kept for overnight. The films formed in $FeCl_3$ solution are blue–black in color which indicates films are fully oxidized. After 24 h, solution was filtered to separate the oligomers and impurities. The product was washed several times with distilled water, acetone followed by drying at room temperature.

Sonochemical Synthesis of CdS Nanoparticles

$$2CdNO_3 + Na_2S \rightarrow CdS + 2NaNO_3$$

Various synthesis methods for preparation of CdS nanoparticles have been reported.[43,49,50] In this work, nanoparticles of CdS was synthesized sonochemically using an ultrasound probe (BO3 Ultrasonic Processor UP1200, Cromtech, India). An excess of 0.5*M* aqueous solution of Na_2S was added dropwise to a 0.005*M* aqueous solution of $CdNO_3$, under ultrasound environment. The temperature of the reaction mixture was maintained at temperature of 30 ± 2^oC. A black precipitate was obtained, which was centrifuged at 8000 rpm, then washed with acetone and water followed by drying in air at temperature of 60^oC.

Preparation of PPy/CdS Nanocomposites by in situ Deposition Polymerization

Various PPy nanoparticles and their nanocomposites incorporated with metal particles have been studied for gas sensing applications.[2–5,11–14,17–20,33–43,48] PPy/CdS nanocomposites[43] were also prepared by in situ chemical polymerization method[14] as shown in Figure 1. Pyrrole was dissolved in distilled water with 0.05*M* of SLS by continuous stirring. Predetermined amount of CdS nanoparticles were dispersed into the pyrrole solution under ultrasound environment. Two pretreated glass slides were placed in the beaker containing pyrrole solution. Polymerization of PPy was facilitated by dropwise addition of aqueous $FeCl_3$ under continuous stirring at ambient temperature (30 ± 1^oC). The molar ratio of $FeCl_3$ to pyrrole was kept at (1 : 2.33). After complete addition of $FeCl_3$, the reaction mixture was stirred for an additional 1 h and then left to stand overnight. Thereafter, the glass slides were taken out of the reaction mixture. Black, uniform films of doped PPy/CdS were deposited on the glass slides; these were washed with water and ethanol and dried for 30 min under vacuum. Then, after 24 h, whole solution was washed with distilled water and ethanol. A black precipitate obtained was then

Figure 2. Gas Sensing Setup. [Color figure can be viewed in the online issue, which is available at wileyonlinelibrary.com.]

dried at room temperature. Different compositions of PPy/CdS nanocomposites were prepared, wherein the amount of CdS nanoparticles was varied as 1, 2, and 3 wt %, and labeled as C1, C2, and C3, respectively.

Preparation of Pellets

To prepare the pellets of PPy and its different nanocomposites the Hydraulic Press Machine (Kimaya Engineering, Mumbai) was used. 0.2 mg of PPy and its different nanocomposites were taken to prepare pellet.

Characterization

Fourier Transform Infrared Spectroscopy. Fourier transform infrared spectroscopy (FTIR) spectra of pure PPy and its different nanocomposites were recorded on Shimadzu FTIR-8400 spectrophotometer (Tokyo, Japan) within the wavenumber range of 400–4000 cm^{-1}. The samples were prepared in the pellet form by mixing with potassium bromide (KBr).

UV-Visible Spectroscopy. UV–vis absorption spectra of pure PPy and its nanocomposites dissolved in distilled water (0.1 mg sample/20 mL DW) were recorded on a Hitachi U-2900 spectrophotometer (Tokyo, Japan) in the range of 200–800 nm.

X-ray Diffraction. X-ray diffraction (XRD) analysis of pure PPy and PPy/CdS nanocomposites (C1, C2, and C3) were conducted on Advance X-ray diffractometer (Brukers D8, Germany) with CuKα1 radiation ($\lambda = 1.5404$ Å).

Field Emission Scanning Electron Microscopy. Field emission scanning electron microscope (FE-SEM; Hitachi S-4800, Tokyo, Japan) was used to assess the surface morphology of powder form of PPy and its different nanocomposites. The samples were given a gold coating and mounted on a specimen stub before viewing under the microscope.

(I–V) Characteristics. The electrical conductivity of various composites was measured by four-point probe conductivity meter method, using a current source (CCS-01) and micro voltmeter (DMV-001, SES Instruments, Scientific Equipments, Roorkee, India).

Measurement of Gas Sensitivity at Room Temperature. Pellets of PPy and its different nanocomposites (C1, C2, and C3) were loaded in a sensing chamber (as shown in Figure 2) and two conducting probes were placed in contact with the pellets. Sensors resistance was measured at interval of 1 s with a programmable 4.5 digital multimeter (SM 5015, Scientific MES-Technik Private Limited, Indore, India) connected to a computer (QT035AV, Hewlett Packard, Bangalore, India) using a RS232C interface that was fully automated and logged by a program.

The (I–V) characteristics of each sample was recorded first in ambient air and then in different concentration of NH_3 and LPG gases (100, 250, and 500 ppm). The electrical resistance of the films was deduced from (I–V) graphs; a change in electrical resistance gave the sensitivity of the pellets to NH_3 and LPG gases. The response of the sensor was measured after a fixed interval of 60 s. All the electrical measurements were taken at room temperature (30 ± 2 °C).

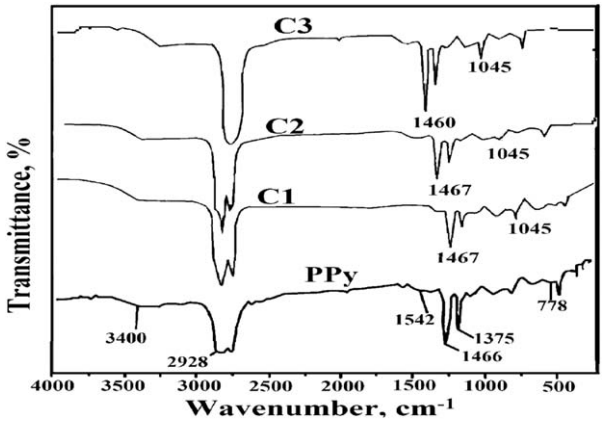

Figure 3. FTIR spectra of PPy and various PPy/CdS nanocomposites.

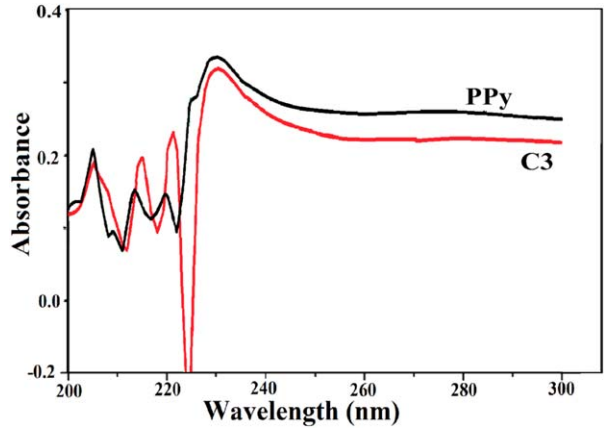

Figure 4. UV absorption of PPy, PPy/CdS composite (C3). [Color figure can be viewed in the online issue, which is available at wileyonlinelibrary.com.]

RESULTS AND DISCUSSION

FTIR

Figure 3 shows functional group presence in PPy and its nanocomposites in all FTIR spectra. For the pristine PPy, the peaks observed at 1542 and 1466 cm^{-1} are related with fundamental vibration of PPy. The broad region at about 3400 cm^{-1} refers to N–H stretching. The peak at 1375 cm^{-1} is related with C–N asymmetric vibration, whereas the peak at 1045 cm^{-1} is related with C–H deformation. The peak at 2928 cm^{-1} associated with C–H stretching vibrations. The band at 1624 cm^{-1} can be assigned for C=C bond. The peak for C–N stretching is at 778 cm^{-1}. It is observed from the spectra [Figure 2(b)] of PPy/CdS nanocomposites for C1 and C2 that the peaks of PPy at 1043 cm^{-1}, 1466 cm^{-1} have shifted to 1045, 1467 cm^{-1}, respectively, are due to the deformation which may have been caused by interaction between CdS and the PPy, and for C3 nanocomposite, the peak 1466 cm^{-1} moved to 1460 cm^{-1}, it may be due to increased amount of CdS in the C3 nanocomposite. The bands from 725 to 615 cm^{-1} show the CdS stretching.

UV-visible Spectroscopy

The UV–vis spectra (Figure 4) show the characteristic peaks of PPy. Pure PPy has weaker absorption for ultraviolet rays ($\lambda < 380$ nm) but stronger absorption for visible light. In PPy, the absorbance was seen at 225 nm. In the case of C3 nanocomposite, these peaks appear shifted to 230 ± 5 nm, as a result of interaction of CdS nanoparticles with PPy chains. No obvious absorbance for CdS nanoparticles can be observed in the spectra due to the agglomeration of the CdS nanoparticles might have affected the UV visible absorption spectrum.

Phase Identification by XRD

Figure 5(a,b) shows the XRD patterns of PPy, CdS nanoparticles, and PPy/CdS nanocomposites. Peak near at 25^0 is associated with (1 1 2) plane of PPy. For the CdS material, the observed peaks have d-values 3.3, 2.8, 2.0, 1.7, and 1.65 nm corresponding to (1 1 1), (2 0 0), (2 2 0), (3 1 1), and (2 2 2) planes, respectively. The crystallite size of these nanoparticles, as calculated by Scherrer's equation, is found to be 84 nm, and the crystallinity is 38.6%.

Figure 5(b) shows the XRD pattern of PPy/CdS nanocomposites shows peaks near at 25^0 which is associated with (1 1 2) plane of PPy. The crystallinity of PPy/CdS nanocomposites (C1, C2, and C3) are 47.4, 43.2, and 42%, respectively. The lowering of crystallinity of C2 and C3 could be due to increase in wt % of CdS nanoparticles. The nanocomposites (C1, C2, and C3) show 52.6, 56.8, and 58% amorphous in nature. The PPy/CdS nanocomposites (C1, C2, and C3) peaks were observed near 27^0, 31^0, and 46^0 associated with (0 1 2), (1 2 0), and (2 2 1) planes, respectively, these planes are associated with CdS nanoparticles.

Surface Morphology of PPy, CdS Nanoparticles, and PPy/CdS Nanocomposites

PPy nanoparticles show almost globular form and a compact grouped growth. Uniform, nanospheres of CdS nanoparticles with a diameter of 60–100 nm is observed in Figure 6(a). Globular shape of PPy can be clearly seen from Figure 6(b). This shows the effectiveness of ultrasound in producing

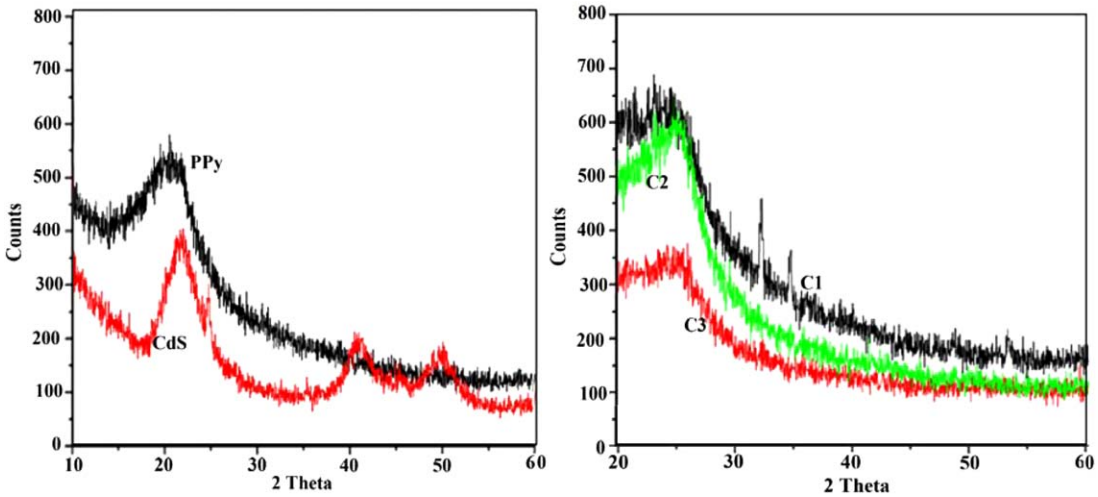

Figure 5. XRD of (a) Pure PPy and CdS nanoparticles, (b) various PPy/CdS nanocomposites. [Color figure can be viewed in the online issue, which is available at wileyonlinelibrary.com.]

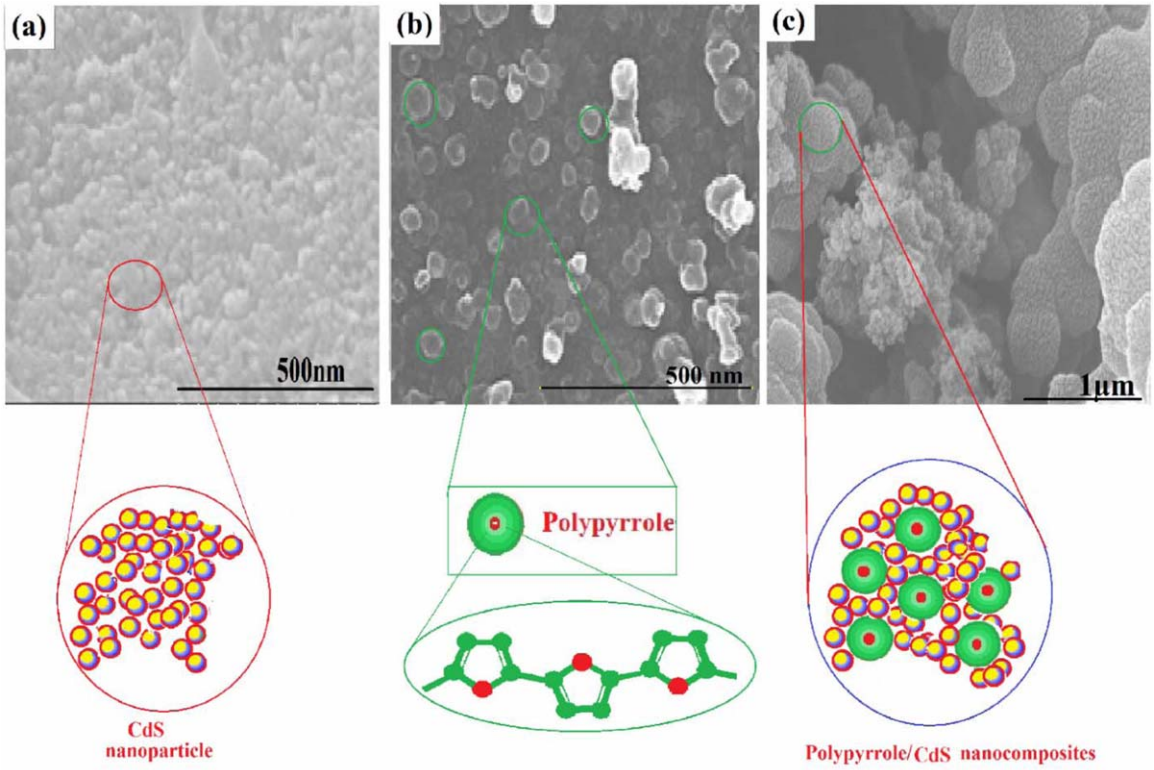

Figure 6. SEM micrographs of (a) CdS nanoparticles, (b) PPy, and (c) PPy/CdS nanocomposites. [Color figure can be viewed in the online issue, which is available at wileyonlinelibrary.com.]

nonaggregated nanoparticles even in the absence of an encapsulating agent. Figure 6(c) shows the nanospheres of CdS to be uniformly dispersed in the PPy matrix. Globular morphology of PPy nanocomposites with a diameter of about 100, 80, and 50 nm (±5 nm) can be seen for C3. From the FE-SEM micrographs, it is evident that ultrasound-induced cavitation produced nonaggregated, nanostructure CdS, and also aided in uniform dispersion of the nanoparticles into the polymer matrix.

(I–V) Characteristics of PPy/CdS Nanocomposites

The electrical conductivities of all pelleted PPy/CdS nanocomposites (C1, C2, and C3) were measured with the help of voltage source and picoammeter. From (I-V) characteristic, it is observed that pristine PPy has an ohmic behavior and thus it behaves like a metal. The conductivity of the PPy/CdS nanocomposites was varied by the addition of CdS nanoparticles. For PPy/CdS nanocomposites, the (I-V) behavior was semiconducting.

Conductivity was observed for pure PPy and its nanocomposites at room temperature. From (I-V) measurements of pristine PPy, the conductivity was recorded as 1.9×10^{-3} S/cm. Here, an increasing trend of conductivity is observed when wt % loading of CdS is increased. But the conductivity of PPy/CdS nanocomposites (C1, C2, and C3) is less than that of PPy as shown in Figure 7. The observed conductivity of PPy/CdS nanocomposites was not greater than PPy but comparison of all three nanocomposites with each other, the conductivity increases by the increasing wt % of CdS nanoparticles. The conductivity of PPy is improved by the addition of different wt % of CdS nanoparticles.[43,49,50] Bohari *et al.*[43] reported conductivity at low and high temperature for these composites.

Sensitivity of PPy/CdS Nanocomposites

All samples were studied to check their reproducibility and absorption and desorption process. The value of relative humidity in test chamber reported by Joshi *et al.*[33] was 50%. Room temperature gas sensing studies were performed for NH_3 and LPG gases using two–probe gas sensing setup (Figure 8). PPy sensors are sensitive with good response to these gases, showing

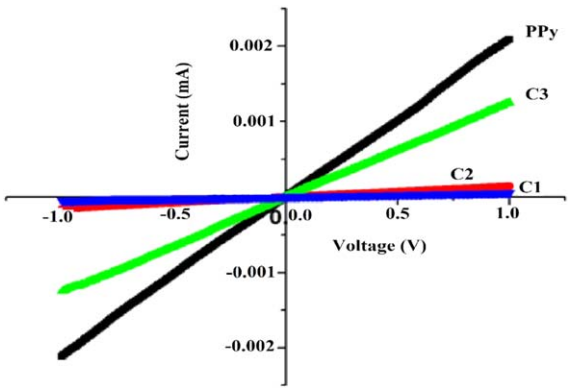

Figure 7. (I-V) characteristics of PPy and PPy/CdS nanocomposites. [Color figure can be viewed in the online issue, which is available at wileyonlinelibrary.com.]

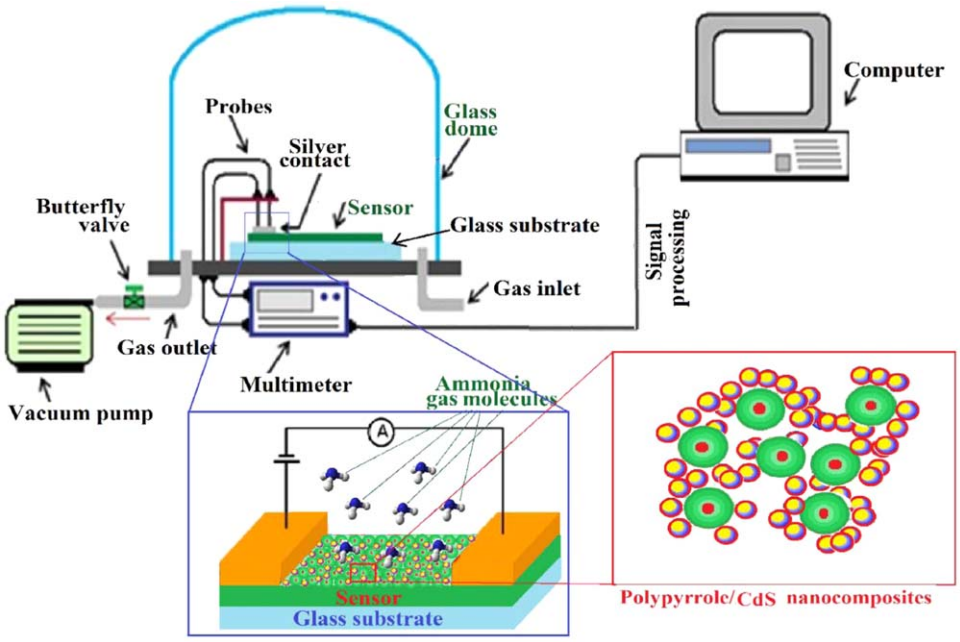

Figure 8. Pictorial representation of a two–probe gas sensing setup. [Color figure can be viewed in the online issue, which is available at wileyonlinelibrary.com.]

larger response to polar than nonpolar compounds. Sensing of NH_3 and LPG gases is useful in many applications like detection of leaks, explosives, fertilizer industries, compressors of air conditioners, breath analysis for medical diagnosis *etc.* Furthermore, its high toxicity also warrants a rapid detection at low concentrations.

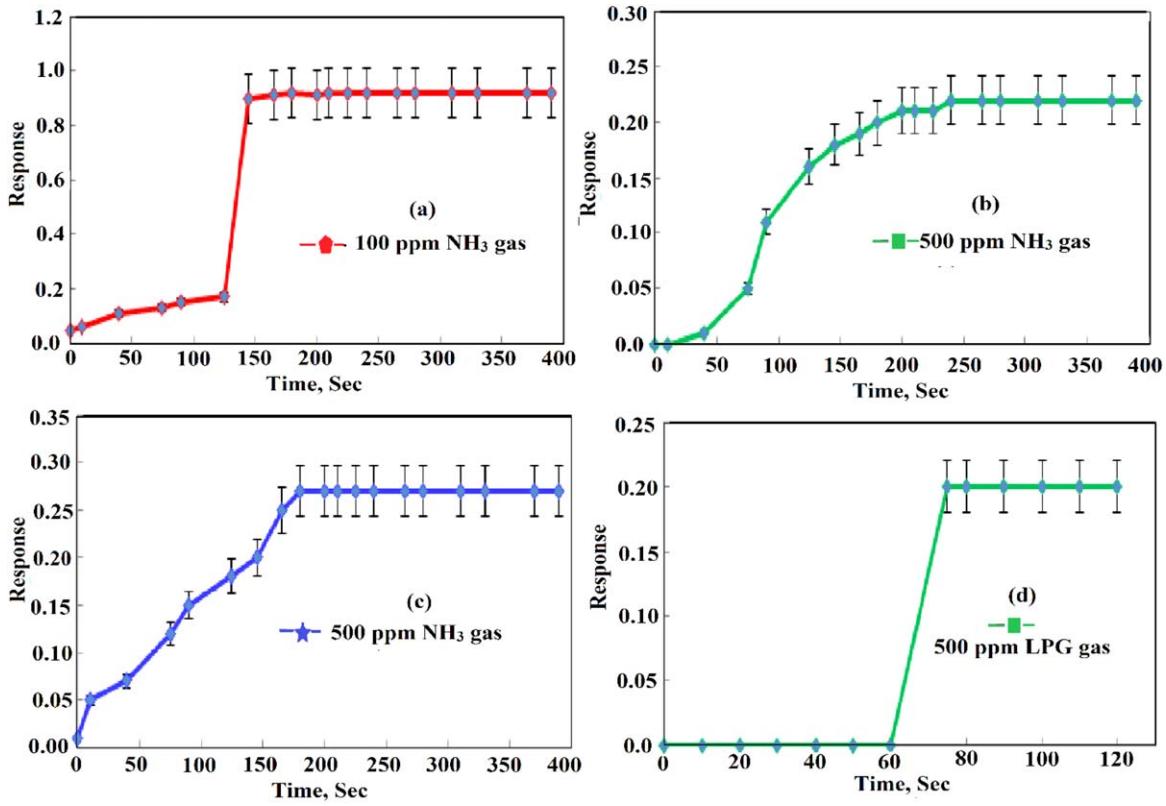

Figure 9. PPy nanoparticles response vs. time for gas sensing of (a–c) NH_3 and (d) LPG. [Color figure can be viewed in the online issue, which is available at wileyonlinelibrary.com.]

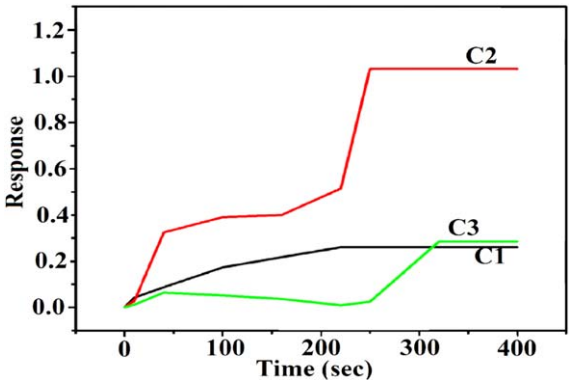

Figure 10. PPy/CdS nanocomposites Response vs. time for sensing of 100 ppm NH_3 gas. [Color figure can be viewed in the online issue, which is available at wileyonlinelibrary.com.]

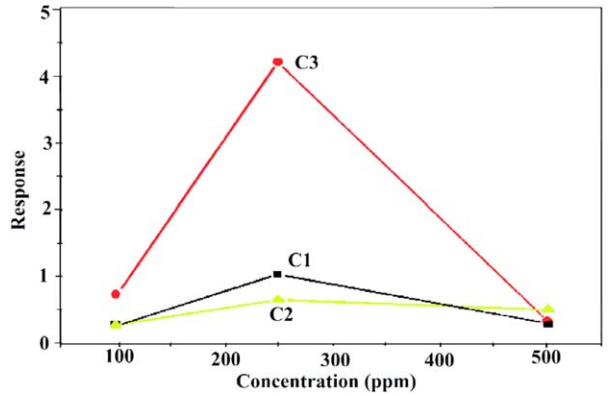

Figure 11. PPy/CdS nanocomposites Response vs. concentration of NH_3 gas. [Color figure can be viewed in the online issue, which is available at wileyonlinelibrary.com.]

For reducing gases like NH_3 and LPG, the resistance of the pellet increases on exposure to the gas. The response of the sensor is given by eq. (1).

$$\text{Response} = (I_a - I_g) / I_a \quad (1)$$

Where, I_a is current in air, I_g is current in gas.

All the PPy/CdS nanocomposites (*i.e.*, C1, C2, and C3) were exposed and studied for detection of NH_3 and LPG gases.

The response curve of PPy at various concentrations of NH_3 and LPG gases showed different curves as shown in Figure 9(a–d). At 100 ppm of NH_3, the decrease in current was higher than at 250 and 500 ppm because of saturation of gas at 250 and 500 ppm. When the NH_3 gas injected in to the chamber, it was absorbed by PPy pellet. As PPy is p-type conductor and NH_3 gas is reducing gas, the electrons from NH_3 gas were accepted by holes in the PPy. As shown in Figure 9(a), pure PPy showed good response at 100 ppm and response value was observed 0.91, but it was suddenly decreased for 250 and 500 ppm as shown in Figure 9(b,c), their values were 0.22 and 0.26, respectively. PPy gave zero response to LPG at 100 ppm but it showed response value 0.2 for the 250 and 500 ppm as shown in Figure 9(d). The response of LPG was less and sensitive, whereas for the NH_3, it was more and effective.

A typical plot of (response vs. time) for all PPy nanocomposites (*i.e.*, C1, C2, and C3) is shown in Figure 10 for NH_3 gas. PPy/CdS nanocomposites (C3) gave nearly zero response (Figure 10) to NH_3 at 100 ppm, but its response value was 0.2 for C1 and observed maximum for C2 (Response = 1.04). C2 nanocomposite shows minimum response time (20 s) with maximum response value (1.04) as compared with C1 and C3 nanocomposites. All PPy nanocomposites (*i.e.*, C1, C2, and C3) showed same resistance and response values were also same for the LPG sensing.

The response curves of all PPy/CdS nanocomposites are shown in Figure 11 at various concentrations of NH_3 gas. At 100 ppm NH_3, the minimum response (Response = <1) was observed for all PPy/CdS nanocomposites, whereas it was observed higher at 250 ppm NH_3 for all PPy/CdS nanocomposites. For C3 nanocomposites, maximum response (4.1) was observed to sense 250 ppm NH_3 gas. It is again decreased for 500 ppm NH_3 gas due to saturation of gas. When the NH_3 gas injected in to the chamber, it get absorbed by PPy pellet. As PPy is p-type conductor and NH_3 is reducing gas, the electrons from NH_3 gas were accepted by holes in the PPy. There was no effect observed for LPG sensing with all these PPy/CdS nanocomposites.

The response for NH_3 was better and faster for all PPy/CdS nanocomposites. A high response for NH_3 indicates selectivity of the pellets toward NH_3 gas. The observed response time for NH_3 was less (20 s) compared with that of LPG (80 s) due to selective sensing of NH_3 gas over LPG. However, the recovery time observed was approximately above 20 min, which was large. The NH_3 response for PPy/CdS nanocomposites is given in Table I.

When $FeCl_3$ doped pure PPy was exposed to NH_3 gas, an increment in current was observed. This is mainly because in chemical preparation of PPy and Cl^- ion is incorporated as counter ion to maintain the electro neutrality. Usually partial oxidation state (up to + 0.33) is produced in the process. In addition, it is observed that some amount of ions remain within the PPy in

Table I. Response of NH_3 at Different Concentration and PPy/CdS Compositions

Composites	Response toward NH3 gas			
	100 ppm	250 ppm	500 ppm	Response time
1% PPy/CdS (C1)	0.26	1.0	0.29	20 s
2% PPy/CdS (C2)	0.28	0.6	0.50	
3% PPy/CdS (C3)	0.74	4.2	0.33	

the Fe^{2+} state. Thus, there is a possibility that higher oxidation state can be induced in the interaction with NH_3. In such a situation, the higher charge on cations can lead to increase in current.

CONCLUSIONS

The characteristic peaks of PPy/CdS nanocomposites synthesized by in situ chemical polymerization were observed by the FTIR and UV-vis spectrums. SEM micrographs showed size and shape of CdS nanoparticles along with their uniform distribution in PPy matrix showing surface morphologies of all PPy/CdS nanocomposites. XRD explained the crystallinity of PPy, CdS nanoparticles and all nanocomposites in which amorphous nature of all PPy nanocomposites was observed. The structural and electrical properties of PPy/CdS polymer nanocomposites showed that the electrical conductivity of PPy is higher than that of PPy/CdS nanocomposites and also the conductivity of the nanocomposite increases with increase in concentration of CdS nanoparticles and hence semiconductor nature improves the conductance of PPy/CdS composites. By using these materials, ammonia gas could be detected efficiently. PPy nanocomposite containing 3 wt % CdS nanoparticles gave higher response (4.1) to sense 250 ppm of NH_3 with 20 s of response time, but it decreased as concentration of NH_3 increased to 500 ppm due to the saturation of NH_3 gas molecules.

ACKNOWLEDGMENTS

Authors are thankful to University Grants Commission, New Delhi, Government of India for providing financial assistance under One Time Grant (UGC-BSR project no.: F.4–10/2010, dated 20 Sept., 2011), Department of Science and Technology (DST-FIST) and UGC (SAP-DRS) to carry out this research work.

REFERENCES

1. Li, X. G.; Hou, Z. Z.; Huang, M. R.; Moloney, M. G. *J. Phys. Chem. C,* **2009**, *113*, 21586.
2. Adhikari, A.; Radhakrishnan, S. *J. Appl. Polym. Sci.* **2011**, *120*, 719.
3. Xie, H. Q.; Liu, C. M.; Guo, J. S. *Polym. Int.* **1999**, *48*, 1099.
4. Wu, T. M.; Chang, H. L.; Lin, Y. W. *Polym. Int.* **2009**, *58*, 1065.
5. Li, X. G.; Li, A.; Huang, M. R.; Liao, Y.; Lu, Y. G. *J. Phys. Chem. C* **2010**, *114*, 19244.
6. Adhikari, B.; Majumdar, S. *Prog. Polym. Sci.* **2004**, *29*, 766.
7. Persaud, K. C. *Mater. Today* **2005**, *8*, 44.
8. Janata, J.; Josowicz, M. *Nature Mater.* **2003**, *2*, 24.
9. Mishra, S.; Shimpi, N. G.; Sen, T. *J. Polym. Res.* **2013**, *20*, 49.
10. Ayad, M. M. *J. Mater. Sci.* **2009**, *44*, 6392.
11. Migahed, M. D.; Fahmy, T.; Ishıra, M.; Barakat, A. *Polym. Test.* **2004**, *23*, 361.
12. Migahed, M. D.; Ishra, M.; Fahmy, T.; Barakat, A. *J. Phys. Chem. Solids* **2004**, *65*, 1121.
13. Yang, C.; Liu, P.; Guo, J.; Wang, Y. *Synth. Met.* **2010**, *160*, 592.
14. Sen, T.; Shimpi, N. G.; Mishra, S. *Sens. Actuators B* **2014**, *190*, 120.
15. Mishra, S.; Ghanshyama, C.; Ram, N.; Bajpai, R. P.; Bedi, R. K. *Sens. Actuators B* **2004**, *97*, 387.
16. de Lacy Costello, B. P. J.; Ewen, R. J.; Ratcliffe, N. M.; Richards, M. *Sens. Actuators B* **2008**, *134*, 952.
17. Chougule, M. A.; Dalavi, D. S.; Sawanta Mali, Patil, P. S.; Moholkar, A. V.; Agawane, G. L.; Kim, J. H.; Sen, S.; Patil, V. B. *Measurement* **2012**, *45*, 1996.
18. Geng, L.; Wu, S. *Mater. Res. Bull.* **2013**, *48*, 4343.
19. Nalage, S. R.; Navale, S. T.; Patil, V. B. *Measurement* **2013**, *46*, 3275.
20. Shumaila, G. B.; Lakshmi, V. S.; Alam, M.; Siddiqui, A. M.; Zulfequar, M.; Husain, M. *Curr. Appl. Phys.* **2011**, *11*, 217.
21. Quercia, L.; Loffredo, F.; Bombace, M.; Girolamo, A. D.; Mauro, D.; Francia, G. D. **2005**, Available at http://www.afs.enea.it/devito/Abstract_Eurosensors/ExtabsEUS05Comp.pdf
22. Sharma, S.; Madou, M. *Philos. Trans. R. Soc. A* **2012**, *370*, 2448.
23. Liu, X.; Cheng, S.; Liu, H.; Hu, S.; Zhang, D.; Ning, H. *Sensor* **2012**, *12*, 9665.
24. Rana, V. K.; Akhtar, S.; Chatterjee, S.; Mishra, S.; Singh, R. P.; Ha, C. S. *J. Nanosci. Nanotechnol.* **2014**, *14*, 2435. Available at http://dx.doi.org/10.1166/jnn.2014.8498.
25. Lu, G.; Xu, J.; Sun, J.; Yu, Y.; Zhang, Y.; Liu, F. *Sens. Actuators B* **2012**, *162*, 88.
26. Trakhtenberg, L. I.; Gerasimov, G. N.; Gromova, V. F.; Belysheva, T. V.; Ilegbusi, O. J. *Sens. Actuators B* **2013**, *187*, 521.
27. Sberveglieri, G. *Sens. Actuators B* **1995**, *23*, 109.
28. Gupta, N.; Sharma, S.; Mir, I. A.; Kumar, D. *J. Sci. Ind. Res.* **2006**, *65*, 557.
29. Tang, H.; Yan, M.; Zhang, H.; Li, S.; Ma, X.; Wang, M.; Yang, D. *Sens. Actuators B* **2006**, *114*, 915.
30. Mani, G. K.; Rayappan, J. B. B. *Sens. Actuators B* **2013**, *183*, 466.
31. Nguyen, L. Q.; Phan, P. Q.; Duong, H. N.; Nguyen, C. D.; Nguyen, L. H. *Sensor,* **2013**, *13*, 1762.
32. Wagh, M. S.; Jain, G. H.; Patil, D. R.; Patil, S. A.; Patil, L. A. *Sens. Actuators B* **2006**, *115*, 133.
33. Joshi, A.; Gangal, S. A.; Gupta, S. K. *Sens. Actuators B* **2011**, *156*, 938.
34. Omastova, M.; Trchova, M.; Kovářova, J.; Stejskal, J. *Synth. Met.* **2003**, *138*, 447.
35. Chitte, H. K.; Bhat, N. V.; Walunj, V. E.; Shinde, G. N. *J. Sens. Technol.* **2011**, *1*, 47.
36. Kemp, N. T.; Kaiser, A. B.; Trodahl, H. J.; Chapman, B.; Buckley, R. G.; Partridge, A. C.; Foot, P. J. S. *J. Polym. Sci. Part B: Polym. Phys.* **2006**, *44*, 1331.
37. Ho, T. A.; Jun, T. S.; Kim, Y. S. *Sens. Actuators B* **2013**, *185*, 523.
38. Han, G.; Shi, G. *Thin Solid Films* **2007**, *515*, 6991.

39. Shen, Y.; Wan, M. *J. Polym. Sci. Part A: Polym. Chem.* **1997**, *35*, 3689.
40. Li, X. G.; Wang, L. X.; Huang, M. R.; Lu, Y. Q.; Zhu, M. F.; Menner, A.; Springer, J. *Polymer* **2001**, *42*, 6095.
41. Lu, X.; Mao, H.; Zhang, W. *Polym. Compos.* **2009**, *30*, 847.
42. King, R. C. Y.; Boussoualem, M.; Roussel, F. *Polymer* **2007**, *48*, 4047.
43. Bohari, N. Z. I.; Talib, Z. A.; Yunos, M. A. S. M.; Anuar, *Int. J. Phys. Sci.* **2012**, *7*, 1670.
44. Tallman, D. E. *J. Solid State Electrochem.* **2001**, *6*, 73.
45. Epstein, A. J. Polyanilines: Recent Advances in Processing and Applications to Welding of Plastics: Intrinsically Conducting Polymers: An Emerging Technology; Kluwer Academic Publisher: Dordrecht, Netherlands, **1993**, 165.
46. MacDiarmid, A. G. The Polyanilines: Potential Technology Based on New Chemistry and New Properties: Science and Applications of Conducting Polymers, **1991**, 117.
47. Harvard 2001, "Energy band gap", homepage. Available at http://people.deas.harvard.edu/~jones/es154/lectures/lecture_2/energy_gap/energy_gap.html. Accessed on 23 February 2006.
48. Li, X. G.; Wang, H. Y.; Huang, M. R. *Macromolecules* **2007**, *40*, 1489.
49. Xi, Y.; Zhou, J.; Guo, H.; Cai, C.; Lin, Z. *Chem. Phys. Lett.* **2005**, *412*, 60.
50. Prabhu, R. *Ind. Acad. Sci. J. Phys.* **2005**, *65*, 801.